Gas Separation

DOI: 10.1002/ange.200602308

Hierarchical Growth of Large-Scale Ordered Zeolite Silicalite-1 Membranes with High Permeability and Selectivity for Recycling CO_2**

Hailing Guo, Guangshan Zhu, Hua Li, Xiaoqin Zou, Xiaoju Yin, Weishen Yang, Shilun Qiu,* and Ruren Xu*

With growing consumption of fossil fuels, gigatons of carbon dioxide are emitted into the atmosphere every year. Carbon dioxide is the main component of greenhouse gases, and would trigger severe global climate change if it accumulated to a high level in the long run. To alleviate CO_2 accumulation it is important to separate and recycle carbon dioxide before it is released in to air.[1] In contrast to conventional techniques for CO_2 separation, membrane gas separation is more affordable and attractive. Recently, polymer membrane materials have been widely used for gas separation owing to their relatively low cost and ease of being processed into hollow fibers.[2–5] However, plasticization could significantly decrease the performance of the polymer membranes. A more promising choice is inorganic zeolite membranes.[6–9] Crystalline silica-based zeolites can bring their intrinsic properties, such as well-defined subnanometer channels, high thermal, chemical, and mechanical stabilities, and hydrophobicity/philicity, into the membrane.

Ideally, zeolite membranes should be large-scale ordered and defect-free, exhibiting high thermal stability, selectivity, and permeability. Zeolite FAU, DDR, T-type, and SAPO-34 membranes have been reported for CO_2/CH_4 and CO_2/N_2 separations. Although these membranes have demonstrated high selectivity for CO_2 over other gas molecules, they have low permeability owing to the thickness of the zeolite films, the random arrangement of zeolite crystals in the membrane,[10] and low thermal and mechanical stabilities because of their high Al contents.[11–13] High silica MFI or pure silica MFI zeolites with 5.3 Å intercross channels have higher thermal stabilities; as a result membranes of them have been considered for xylene isomer separation in the petrochemical industry.[14] Zeolite MFI membranes supported by, for example, porous ceramic, α-Al_2O_3, and stainless steel have many defects, such as pinholes or cracks, which are usually generated through different thermal-expansion coefficients and phase transitions between the membranes and matrices.[15–17] Some defect-free MFI films have been reported.[18] Considering the elasticity, tenacity, and low thermal-expansion coefficient of the stainless-steel-net, it is reasonable to expect that a stainless-steel-net-imbedded zeolite silicalite-1 membrane can resist cracking, temperature cycling, and possess high mechanical stability. Based on the preparation of a stainless-steel-net-supported zeolite NaA membrane,[19] the investigation of a large-scale ordered stainless-steel-net-imbedded zeolite silicalite-1 membrane was carried out. Mixed gas (N_2/CO_2, CH_4/CO_2, and H_2/CO_2) separation studies on the membrane revealed that the membrane has high permeability and selectivity for CO_2 over H_2, N_2,and CH_4.

The stainless-steel-net-imbedded zeolite silicalite-1 membrane was synthesized by the hydrothermal method. First, the silicalite-1 nanocrystal seeds were dispersed onto the pretreated stainless-steel net. The monolayer seeded net was then placed vertically in a Teflon-lined autoclave containing a reaction solution of 0.32 TPAOH/1.0 TEOS/165 H_2O (TPAOH = tetrapropylammonium hydroxide, TEOS = tetraethylorthosilicate) for secondary growth at 170 °C for 3 days.

Figure 1 shows the X-ray diffraction (XRD) patterns of the dispersed seeds on the substrate and as-synthesized zeolite silicalite-1 membranes after secondary growth for 1, 2, and 3 days. The pattern of the dispersed zeolite silicalite-1 seeds fits well with that of the simulated MFI structure, indicating that the sample was a pure phase. The XRD pattern in Figure 1b shows that after reaction for 1 day, the majorities of peaks were similar to those of a randomly oriented MFI structure, except that the intensities of the (*h*0*l*) peaks increased notably, implying the zeolite crystals are (*h*0*l*) oriented on the stainless steel net. When the reaction time was

[*] H. Guo, Prof. G. Zhu, H. Li, X. Zou, X. Yin, Prof. S. Qiu, R. Xu
State Key Laboratory of Inorganic Synthesis and Preparative Chemistry, College of Chemistry
Jilin University
Changchun 130012 (China)
Fax: (+86) 431-516-8331
E-mail: zhugs@mail.jlu.edu.cn
sqiu@mail.jlu.edu.cn
Prof. W. Yang
State Key Laboratory of Catalysis
Dalian Institute of Chemical Physics
Chinese Academy of Sciences
Dalian 116023 (China)

[**] We are grateful for the financial support of the State Basic Research Project (2006CB806100) and the National Natural Science Foundation of China (Grant nos. 20571030, 20531030, and 20371020).

Supporting information for this article is available on the WWW under http://www.angewandte.org or from the author.

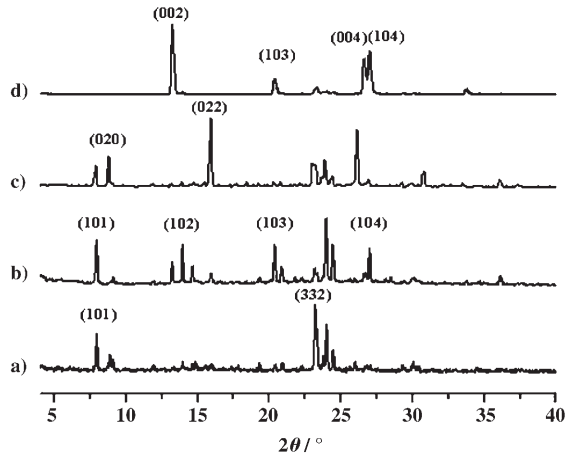

Figure 1. X-ray diffraction patterns of a) the zeolite silicalite-1 nanocrystal seeded substrate and the as-synthesized stainless-steel-net-supported zeolite silicalite-1 membrane after crystallization for b) 1, c) 2, or d) 3 days.

prolonged to 2 days, the intensities of the (020) peak located at a Bragg angle 2θ of 8.8° significantly increased, indicating that at this time the membrane was formed preferentially along the *b* axis (Figure 1c). After 3 days' crystallization, the peaks (101) and (020) (Figure 1d) disappear entirely while the (002), (004), (103), and (104) peaks dominate the XRD pattern, indicating that a *c*- and (*h*0*l*)-oriented zeolite silicalite-1 film has formed on the previously grown *b*-oriented zeolite layer.

To further understand the formation mechanism of the stainless-steel-net-imbedded zeolite silicalite-1 membrane, scanning electron microscopy (SEM) was used to monitor the surface morphology of the zeolite membrane during the synthesis process. As shown in Figure 2a,b, the zeolite silicalite-1 seeds around 150 nm in size were dispersed uniformly on the stainless steel net to form a compact monoseed layer. The lack of close-packed seeds on the net can lead to formation of dome-like defects,[20] which will further affect the gas separation performance of the membrane. The use of zeolite seeds will promote both the nucleation and growth of zeolite on the substrate.[21] The process of the secondary growth of the zeolite silicalite-1 membrane on the seeded substrate is shown in Figure 2c–h. It can be seen that after crystallization for 1 day (Figure 2c,d), most of the crystals grow along the stainless steel net wire to form a zeolite fiber net, consisting with the XRD results (Figure 1b). The formation of the zeolite fiber net with a preferred crystallographic orientation can be explained by a classic competitive growth model.[22–24] Figure 2e shows the image of the zeolite membrane grown after two days. At this stage, there are still many voids where zeolite crystals can not merge into a membrane. It can be seen that as crystallization progresses, the 40×50 μm rectangle pores constructed by zeolite fibers developed into 20×30 μm elliptic pores. The magnified SEM image of one elliptic pore (Figure 2f) clearly indicates that zeolite film is made up of two layers of zeolite crystal arrays. The prismatic crystals in the first layer are parallel to the plane of the net, with their *c*-axes pointing

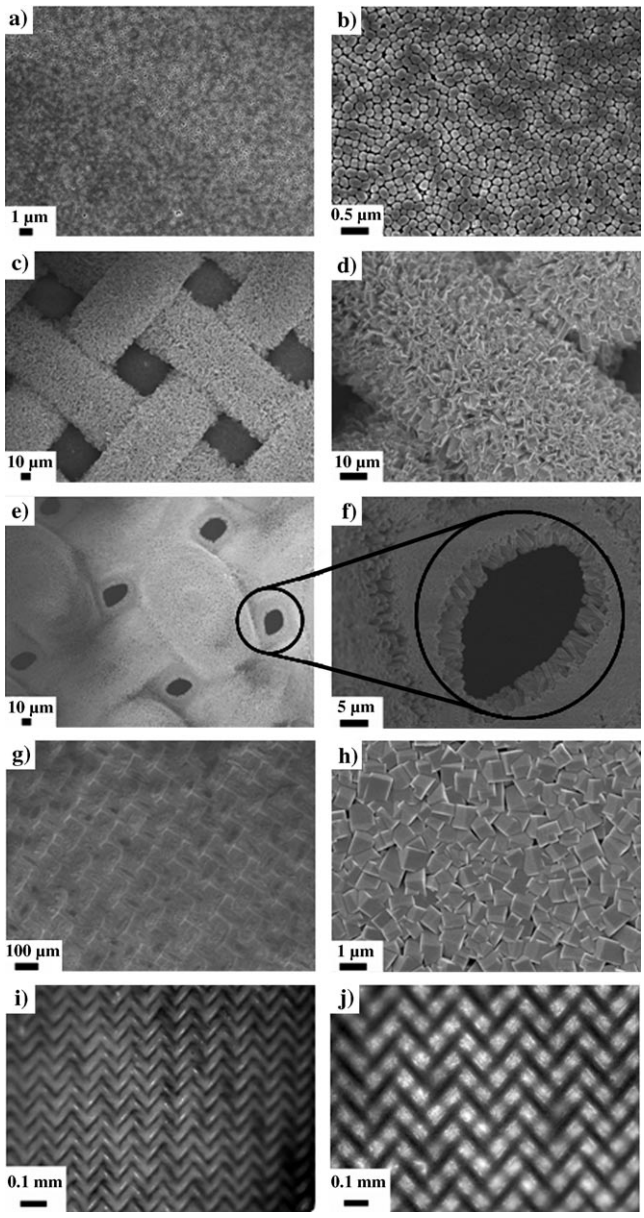

Figure 2. SEM images of a) the zeolite silicalite-1 nanocrystal seeds dispersed on the net wafer, and b) magnified image of the seed layer. Top-view SEM images of stainless-steel-net-supported zeolite silicalite-1 membrane after secondary growth with crystallization times of c,d) 1 day, e,f) 2 days, and g,h) 3 days, under low (left) and high (right) magnification. i,j) Optical microscope images of the membrane with reflected and transmitted light.

towards the center of the elliptic pores. Without space restriction, these crystals grew expitaxially and merged together.[25,26] The crystals in the second layer are grown over the first layer with their *c*-axes perpendicular to the plane of the net. Only those crystals with *c*-axes perpendicular to the substrate surface will survive, whereas those with other orientations are gradually suppressed.[27] Such an arrangement of zeolite crystals fits well with the XRD result (Figure 1c). After crystallization for 3 days, as shown in the Figure 2g, an entirely compact and continuous zeolite silicalite-1 membrane without any pinholes or cracks was synthe-

sized successfully. The magnified SEM image (Figure 2h) indicates that almost all the crystals are in the *c* orientation with their *c* axis perpendicular to the plane of the membrane, which is consistent with the result of XRD pattern (Figure 1d) which shows that crystals prefer the (0*k*0) orientation. Optical microscope images of the membrane with reflected and transmitted light (Figure 2i,j) show that the zeolite net is uniform, ordered over a large area, and transparent. After calcination at 550 °C in air for 8 h, the membrane still retains its high crystallinity and pure phase, which is demonstrated by XRD and SEM analyses (see Supporting Information). It was noted that the thermal expansion coefficients of stainless steel ($15\times10^{-6}\,°C^{-1}$) and the zeolite crystals in the *c* direction ($0.5\times10^{-6}\,°C^{-1}$) are quite small, while the thermal expansion coefficients of zeolite crystals in the *a* and *b* directions are opposing (20×10^{-6} and $-22\times10^{-6}\,°C^{-1}$, respectively). It has been reported that the in-plane compressive stress may prevent crack formation.[28] Therefore, we speculate that it was the hierarchical (that is, layer-by-layer) structure of the zeolite membrane that enabled it to survive the high-temperature calcination process without cracking or formation of pinholes.

Following the encouraging characterization results, gas-separation studies were carried out on the high thermal stable and large-scale ordered silicalite-1 membrane. The calcined membrane was fixed in a gas-separation setup (see Supporting Information), and used for separation studies with different gas mixtures (CO_2/H_2, CO_2/N_2, and CO_2/CH_4). The determined permeation and separation factors are summarized in the Supporting Information. The permeation of CO_2 (around $7\times10^{-7}\,mol\,m^{-2}\,s^{-1}\,Pa^{-1}$) is much higher than that of the other gases in the mixtures, showing that the membrane provides highly selective separation of CO_2. Because CO_2 has a larger quadrapolar moment and higher boiling point (−44 °C) than the other test gas molecules, it can interact with the interior of the silicalite-1 micropore upon instant polarization, and was adsorbed into and diffused out of the silicalite-1 membrane much more easily than H_2, N_2, and CH_4. Furthermore, the stainless-steel-net has open voids and the first layer of the membrane is almost *b*-oriented which facilitates easy access to the straight-channels of zeolite silicalite-1, as a result the CO_2 permeation factors are much higher than those reported to date.[29–31] In the Supporting Information, it is also noted that the separation factors of mixture gas are much higher than the ideal separation factors. It can be deduced that the preferred adsorption of CO_2 blocks the flow of N_2, H_2, CH_4 molecules through the zeolite silicalite-1 channels of the membrane.[32,33]

To evaluate the mechanical stability of the zeolite membrane, the feed pressure was increased from 1.01×10^5 Pa to 3×10^5 Pa. It is found that the CO_2 permeability increased from 7.14×10^{-7} to $1.53\times10^{-6}\,mol\,m^{-2}\,s^{-1}\,Pa^{-1}$ and the separation factor of CO_2/N_2 still maintained a high value (Supporting Information). Interestingly, the CO_2/N_2 separation factor of the zeolite membrane increased noticeably from 68.7 to 75.0 when the permeation temperature decreased from 20 to 0 °C, suggesting that at lower temperature the adsorption of CO_2 on the zeolite silicalite-1 membrane is more selective than of N_2, H_2, and CH_4. The reproducibility and durability of the membranes were also examined. As shown in Figure 3, the separation factor and the permeation of the zeolite silicalite-1 membrane remains at high values. The membrane can be used repeatedly for at least six months, which shows that the stainless-steel-net-imbedded zeolite silicalite-1 membrane has significantly high stability.

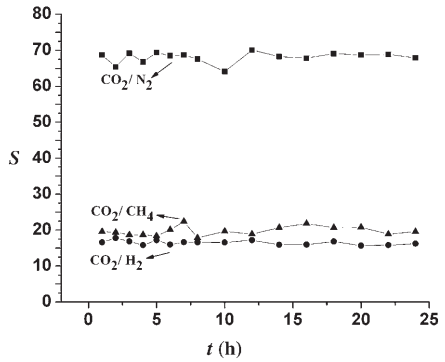

Figure 3. CO_2/N_2 (■), CO_2/H_2 (●), and CO_2/CH_4 (▲) separation factors (*S*) for the stainless-steel-net-supported zeolite silicalite-1 membrane over time; sweep rate = 50 ml min^{-1}, feed flow rate = 100 ml min^{-1}, feed pressure = 1.0×10^5 Pa, permeation temperature = 20 °C.

In summary, the stainless-steel-net-imbedded silicalite-1 zeolite membrane has been successfully synthesized by a hydrothermal approach. A hierarchical growth mechanism for the membrane formation can be deduced according to the XRD and SEM results. Compared with the conventional MFI membranes supported by other substrates, the stainless-steel-net-imbedded zeolite silicalite-1 membrane has high thermal and mechanical stabilities, large-scale order, and exhibits high permeation flux and excellent permeation selectivity for CO_2. Such highly efficient zeolite membranes could be used to separate, recycle, and reuse CO_2 exhaust gases from coal-fired power plants, chemical factories, and natural gas-sourced amine plants.

Experimental Section

Seeds dispersion and hierarchical growth: Silicalite-1 crystals of approximately 150 nm in size were prepared according to literature methods.[34] The seed solution (20 g L^{-1}) was prepared by adjusting the pH value to 10 using aqueous NH_3 to avoid the seed aggregation. Then the seed solution was dropped onto the net wafers which had been pretreated with a liquid detergent solution for 30 min under ultrasonic vibration condition.[16] The seeded net wafers were placed vertically in a Teflon-lined autoclave for secondary growth at 170 °C for 3 days, in which the composition of the reaction solution was 0.32 TPAOH/1.0 TEOS/165 H_2O.[35] To study the growth mechanism of membranes, autoclaves were taken out at 1, 2, and 3 days, respectively. The membranes were taken out, washed with distilled water, and dried at 80 °C. After being calcined at 550 °C for 8 h to remove the organic template, the membranes were characterized by XRD and SEM, and their gas-separation properties were determined.

The growth process of the membrane was monitored by X-ray diffraction (XRD, a Siemens D5005 diffractometer with $Cu_{K\alpha}$ radiation ($\lambda = 1.5418$ Å) and field-emission scanning electron microscope (FE-SEM: JEOS JSM 6700F). A soap-film flow meter was used

to measure the flux of the gas, and the gas that penetrated through the membrane was analyzed by gas chromatograph (HP6890).

Received: June 9, 2006
Published online: October 2, 2006

Keywords: carbon dioxide · gas separation · hierarchical growth · membranes · zeolites

[1] R. F. Service, *Science* **2004**, *305*, 962.
[2] H. Lin, E. V. Wagner, R. Raharjo, B. D. Freeman, I. Roman, *Adv. Mater.* **2006**, *18*, 39.
[3] W. Xu, P. Blazkiewicz, S. Fleming, *Adv. Mater.* **2001**, *13*, 1014.
[4] L. Liu, A. Chakma, X. Feng, *Ind. Eng. Chem. Res.* **2005**, *44*, 6874.
[5] A. S. Kovvali, H. Chen, K. K. Sirkar, *J. Am. Chem. Soc.* **2000**, *122*, 7594.
[6] J. Caro, M. Noack, P. Kölsch, R. Schäfer, *Microporous Mesoporous Mater.* **2000**, *38*, 3.
[7] A. Tavolaro, E. Drioli, *Adv. Mater.* **1999**, *11*, 975.
[8] T. C. Bowenl, R. D. Noble, J. L. Falconer, *J. Membr. Sci.* **2004**, *245*, 1.
[9] M. C. Lovallo, A. Gouzinis, M. Tsapatsis, *AIChE J.* **1998**, *44*, 1903.
[10] T. Tomita, K. Nakayama, H. Sakai, *Microporous Mesoporous Mater.* **2004**, *68*, 71, and reference therein.
[11] Y. Cui, H. Kita, K. Okamoto, *J. Mater. Chem.* **2004**, *14*, 924.
[12] a) X. Gu, J. Dong, T. M. Nenoff, *Ind. Eng. Chem. Res.* **2005**, *44*, 937; b) K. Kusakabe, T. Kuroda, K. Uchino, Y. Hasegawa, S. Morooka, *AIChE J.* **1999**, *45*, 1220.
[13] a) S. Li, J. G. Martinek, J. L. Falconer, R. D. Noble, *Ind. Eng. Chem. Res.* **2005**, *44*, 3220; b) J. C. Poshusta, V. A. Tuan, J. L. Falconer, R. D. Noble, *Ind. Eng. Chem. Res.* **1998**, *37*, 3924.
[14] a) W. Yuan, Y. S. Lin, W. Yang, *J. Am. Chem. Soc.* **2004**, *126*, 4776, and reference therein; b) G. Xomeritakis, Z. Lai, M. Tsapatsis, *Ind. Eng. Chem. Res.* **2001**, *40*, 544.
[15] F. Z. Zhang, M. Fuji, M. Takahashi, *Chem. Mater.* **2005**, *17*, 1167.
[16] W. Dong, Y. Long, *Chem. Commun.* **2000**, 1067.
[17] J. Dong, Y. S. Lin, M. Z. C. Hu, R. A. Peascoe, E. A. Payzant, *Microporous Mesoporous Mater.* **2000**, *34*, 241.
[18] G. Xomeritakis, M. Tsapatsis, *Chem. Mater.* **1999**, *11*, 875, and reference therein.
[19] X. Yin, G. Zhu, W. Yang, Y. Li, G. Zhu, R. Xu, J. Sun, S. Qiu, R. Xu, *Adv. Mater.* **2005**, *17*, 2006.
[20] G. Xomeritakis, A. Gouzinis, S. Nair, T. Okubo, M. He, R. M. Overney, M. Tsapatsis, *Chem. Eng. Sci.* **1999**, *54*, 3521.
[21] J. Choi, S. Ghosh, Z. Lai, M. Tsapatsis, *Angew. Chem.* **2006**, *118*, 1172; *Angew. Chem. Int. Ed.* **2006**, *45*, 1154.
[22] A. J. Bons, P. D. Bons, *Microporous Mesoporous Mater.* **2003**, *62*, 9.
[23] A. Gouzinis, M. Tsapatsis, *Chem. Mater.* **1998**, *10*, 2497.
[24] R. Xu, G. Zhu, X. Yin, X. Wan, S. Qiu, *Microporous Mesoporous Mater.* **2006**, *90*, 39.
[25] J. Sun, G. Zhu, X. Yin, Y. Chen, Y. Cui, S. Qiu, *Chem. Commun.* **2005**, 1070.
[26] a) H.-K. Jeong, J. Krohn, K. Sujaoti, M. Tsapatsis, *J. Am. Chem. Soc.* **2002**, *124*, 12966; b) T. Okubo, T. Wakihara, J. Plévert, S. Nair, M. Tsapatsis, Y. Ogawa, H. Komiyama, M. Yoshimura, M. E. Davis, *Angew. Chem.* **2001**, *113*, 1103; *Angew. Chem. Int. Ed.* **2001**, *40*, 1069.
[27] G. Bonilla, D. G. Vlachos, M. Tsapatsis, *Microporous Mesoporous Mater.* **2001**, *42*,191.
[28] H. Jeong, Z. Lai, M. Tsapatsis, J. C. Hanson, *Microporous Mesoporous Mater.* **2005**, *84*, 332, and reference therein.
[29] W. Zhu, P. Hrabanek, L. Gora, F. Kapteijn, J. A. Moulijn, *Ind. Eng. Chem. Res.* **2006**, *45*, 767.
[30] D. W. Shin, S. H. Hyun, C. H. Cho, M. H. Han, *Microporous Mesoporous Mater.* **2005**, *85*, 313.
[31] S. Aguado, A. C. Polo, M. P. Bernal, J. Coronas, J. Santamaría, *J. Membr. Sci.* **2004**, *240*, 159.
[32] a) W. J. W. Bakker, F. Kapteijn, J. Poppe, J. A. Moulijn, *J. Membr. Sci.* **1996**, *117*, 57; b) Z. A. E. P. Vroon, K. Keizer, M. J. Gilde, H. Verweij, *J. Membr. Sci.* **1998**, *144*, 65.
[33] J. M. Graaf, E. Bijl, A. Stol, F. Kapteijn, J. A. Moulijn, *Ind. Eng. Chem. Res.* **1998**, *37*, 4071.
[34] G. Zhu, S. Qiu, F. Gao, D. Li, Y. Li, R. Wang, B. Gao, B. Li, Y. Guo, R. Xu, Z. Liu, O. Treasaki, *J. Mater. Chem.* **2001**, *11*, 1687.
[35] Z. B. Wamg, Y. Yan, *Chem. Mater.* **2001**, *13*, 1101.

